Timpmann, K., Jalviste, E., Chenchiliyan, M., Kangur, L., Jones, M. R., & Freiberg, A. (2020). High Pressure Tuning Of Primary Photochemistry In Bacterial Photosynthesis: Membrane-bound Versus Detergent-isolated Reaction Centers. *Photosynthesis Research*, *2020*. https://doi.org/10.1007%2Fs11120-020-00724-z

High Pressure Tuning Of Primary Photochemistry In Bacterial Photosynthesis: Membrane-bound Versus Detergent-isolated Reaction Centers

Kõu Timpmann[a], Erko Jalviste[a], Manoop Chenchiliyan[a], Liina Kangur[a], Michael R. Jones[b], and Arvi Freiberg[a, c, d] *

[a]Institute of Physics, University of Tartu, W. Ostwald Str. 1, Tartu 50411, Estonia

[b]School of Biochemistry, University of Bristol, Biomedical Sciences Building, University Walk, Bristol, BS8 1TD, United Kingdom

[c]Institute of Molecular and Cell Biology, University of Tartu, Riia 23, Tartu 51010, Estonia

[d]Estonian Academy of Sciences, Kohtu 6, 10130 Tallinn, Estonia

*__Corresponding author__: Tel: +37256453175, e-mail: arvi.freiberg@ut.ee

ABSTRACT: While photosynthesis thrives at close to normal pressures and temperatures, it is presently well known that life is similarly commonplace in the hostile environments of the deep seas as well as around hydrothermal vents. It is thus imperative to understand how key biological processes perform under extreme conditions of high pressures and temperatures. Herein, comparative steady-state and picosecond time-resolved spectroscopic studies were performed on membrane-bound and detergent-purified forms of a YM210W mutant reaction center (RC) from *Rhodobacter sphaeroides* under modulating conditions of high hydrostatic pressure applied at ambient temperature. A previously established breakage of the lone hydrogen bond formed between the RC primary donor and the protein scaffold was shown to take place in the membrane-bound RC at an almost 3 kbar higher pressure than in the purified RC, confirming the stabilizing role of the lipid environment for membrane proteins. The main change in the multi-exponential decay of excited primary donor emission across the experimental 10 kbar pressure range involved an over two-fold continuous acceleration, the kinetics becoming increasingly mono-exponential. The fastest component of the emission decay, thought to be largely governed by the rate of primary charge separation, was distinctly slower in the membrane-bound RC than in the purified RC. The change in character of the emission decay with pressure was explained by the contribution of charge recombination to emission decreasing with pressure as a result of an increasing free energy gap between the charge-separated and excited primary donor states. Finally, it was demonstrated that, in contrast to a long-term experimental paradigm, adding a

combination of sodium ascorbate and phenazine methosulfate to the protein solution potentially distorts natural photochemistry in bacterial RCs.

INTRODUCTION

In photosynthesis, solar energy is converted into chemical energy by a sequence of light-driven electron transfer (ET) steps in a transmembrane pigment–protein complex called the reaction center (RC). The accumulated potential energy of separated electrical charges across the membrane dielectric is then used to drive all subsequent cellular processes, thereby powering most of the biosphere (Blankenship 2002). In the wild-type RC from the purple photosynthetic bacterium *Rhodobacter* (*Rba.*) *sphaeroides* (Williams et al. 1986), charge separation takes place on a time scale of a few picoseconds between a primary electron donor (*P*) formed from two closely interacting bacteriochlorophyll (BChl) molecules (P_A and P_B—the so-called special pair) and a quasi-monomeric BChl acceptor (B_A). The electron is then passed to a bacteriopheophytin (BPhe–H_A) and onward to a primary (Q_A) and then secondary ubiquinone acceptor (Q_B) (Hoff and Deisenhofer 1997).

The mechanism of this highly quantum-efficient charge separation has been studied using wide range of spectroscopic and related techniques, with valuable contributions from site-directed mutagenesis to alter the protein structure or cofactor composition and to modulate radical pair lifetimes (Hunter et al. 2008). Most of this extensive research, which has elevated bacterial RCs into the ranks of the best studied membrane proteins, has been performed on detergent-purified complexes, while only a few studies on RCs in functional membranes exist. Yet evidence is mounting that many photosynthetic processes proceed significantly differently in the membrane environment (Freiberg et al. 2012,2016; Beekman 1997,1995; Pflock 2008; Urboniene 2007; Timpmann et al. 2000; Bowyer 1985; Hunter et al. 1985; Driscoll 2014; Pugh et al. 1998).

The present work was aimed at systematically comparing the spectral and kinetic properties of a RC at ambient temperature when housed in either an artificial detergent micelle or a lipid bilayer membrane. To modulate and enhance effects of the environment, a high hydrostatic pressure reaching 10 kbar (1 GPa) was applied. Pressure as a thermodynamic parameter is known to control general physical properties of proteins (Scharnagl et al. 2005). It acts on a sample volume, favoring states with a smaller volume (Scharnagl et al. 2005; Silva and Weber 1993; Boonyaratanakornkit et al. 2002). A protein is destabilized by applied pressure if

the partial molar volume of its denatured state is smaller than that of the respective native state. In the light-harvesting and RC complexes of photosynthetic bacteria, rather specific local effects have also been observed following high-pressure compression such as major modifications of the binding pockets of pigment cofactors and the breakage of hydrogen (H–) bonds that coordinate pigments to the surrounding protein scaffold (Kangur et al. 2008,2017; Freiberg 2012). A useful parallel is water, where the network of H-bonds either in the liquid or solid phase weakens (Jonas et al. 1976) or becomes totally destroyed (as in ice) upon high-pressure compression. Yet membrane proteins appear even more complex constructs than water. In aqueous solution the lipophilic transmembrane helix domain of a membrane protein is protected by a two-dimensional assembly of lipid molecules that form a bilayer. On purification the lipid bilayer is replaced by a belt-like assembly of detergent molecules. In both cases, the hydrophilic N- or C-termini of the membrane-spanning helices are exposed to solvent phase. The interfacial protein areas are supposed to determine the reaction of the protein to changing pressure. In photosynthetic pigment–protein complexes, these effects can be sensitively monitored by changes in the line shapes of pigment optical spectra (Pajusalu et al. 2019).

Efforts to study effects of high pressure on the spectral or kinetic properties of RCs at physiological temperatures have been relatively rare (Kangur et al. 2017; Clayton and Devault 1972; Windsor and Menzel, 1989; Redline et al. 1991; Redline and Windsor 1992; Gall 2001,2004; Leiger 2007; Timpmann 2017; Timpmann et al. 1998; Freiberg 1993). Part of the challenge has been (and still is) the very short singlet excited state lifetime of the special pair in the wild-type RC, and as a consequence, its rather low emission quantum yield. Therefore, in this work, we utilized an engineered YM210W RC from *Rba. sphaeroides*, in which a tyrosine (Y) residue at position M210 was replaced by a tryptophan (W), see Fig. 1a. This well- characterized (McAuley 2000; Nagarajan 1993; Beekman 1996; Pawlowicz 2010; Dominguez 2014) RC modification slows the primary charge separation rate by more than 20-fold, creating a situation where the expected pressure-induced acceleration of this process can be conveniently studied by a commercial picosecond time-correlated single-photon counting system (see Materials and Methods) over broad pressure range. Two facts about the YM210W RC are of special importance with respect to this work. First, as for the wild-type RC, there is only a single modulating H-bond between the special pair (specifically P_A) and its protein surroundings (Fig. 1a). Second, in the YM210W RC, the primary charge separation rate decreases with lowering temperature (Nagarajan et al. 1993), suggesting a thermally activated ET. This is in contrast to the activation-less ET displayed by the wild-type RC, where the rate increases when the temperature decreases (Hoff and Deisenhofer 1997).

Two types of sample were investigated in this work. The first comprised YM210W RCs expressed in a strain of *Rba. sphaeroides* that lacks the LH1 and LH2 antenna complexes, leaving the RC as the sole bacteriochlorophyll-containing protein in the photosynthetic membrane (Jones et al. 1992a,1992b). In such membranes, the RC is no longer surrounded by the native LH1 complex, but it is embedded in a bilayer comprising native *Rba. sphaeroides* lipids. Such antenna-free RCs are fully functional (Beekman 1996; Jones 1992a,1992b; Schmidt et al. 1993) and capable of supporting photosynthetic growth if a sufficiently high light intensity is supplied (Fulcher et al. 1998). This type of membrane-embedded *Rba. sphaeroides* RC, both wild-type and altered through mutation, has been used previously to study multiple aspects of photochemical charge separation and charge recombination (e.g., see (Beekman 1995; Beekman 1996; Vos 1994a; Vos 1994b; Brederode et al. 1997; Brederode 1997; Brederode 1999; Gibasiewicz 2011; Gibasiewicz 2013; Gibasiewicz 2016)). The second type of sample comprised YM210W RCs purified from such membranes using detergent.

In natural photosynthesis, the special pair remains in an oxidized (P^+) state for a considerable amount of time following charge separation and so is unable to accept further excitations. This defines the closed RC state. Subsequent reduction of the special pair via a cyclic electron transfer mechanism reactivates the RC with a typical rate of 10 s^{-1} (Müller et al. 1996). To accelerate reduction of the special pair, and thereby improve the signal during in vitro measurements, external electron donors such as ascorbate are frequently used, often in combination with a one-electron redox mediator such as phenazine methosulfate (PMS). Then, under intense photo-excitation, electrons start readily accumulating on the primary and secondary ubiquinone acceptors. It is widely believed, though, that this latter effect does not interfere with the primary photochemistry processes in the RC. To check this postulate, experiments in the present work were performed in both the absence and presence of sodium ascorbate and PMS. In their absence the excitation light intensity was kept sufficiently low to avoid light-induced closing of the RCs, as first systematically studied in intact bacterial membranes complete with light-harvesting and RC complexes by Borisov et al. (Borisov et al. 1984; Godik and Borisov 1980,1979; Borisov 1985).

The current research showed that although steady-state spectral differences between YM210W RCs embedded in a detergent micelle or in a bilayer formed from native lipids were relatively small, essential differences in emission kinetics and protein stability properties were observed on the application of pressure. It was also concluded that treatment with sodium ascorbate and PMS has several spectroscopic effects due to changes in the primary

photochemistry of the RC, overturning the long-standing experimental conjecture outlined above.

MATERIALS AND METHODS

Samples

Bacterial cells were grown in M22 + medium under dark/semiaerobic conditions (Jones et al. 1992a,1994). For membranes, harvested bacterial cells were resuspended in 20 mM Tris (pH 8.0) and lysed at 20,000 psi in a Constant Systems Cell Disruptor in the presence of DNase. Debris was removed by centrifugation (18,000 rpm, 4 °C, 20 min) and membranes in the supernatant layered onto a density gradient formed from equal volumes of 40% and 15% (w/v) sucrose in 20 mM Tris (pH 8.0). Gradients were ultracentrifuged (38,000 rpm, 4 °C, 2 h) and membranes harvested from the interface between the 15% and 40% sucrose layers. These were diluted in 20 mM Tris (pH 8.0) and concentrated by ultracentrifugation in tubes with a cushion of 60% (w/v) sucrose in 20 mM Tris (pH 8.0) at the bottom (~ 15% of tube volume) to prevent pelleting that might cause membrane aggregation. After ultracentrifugation (38,000 rpm, 4 °C, 1 h), the band of concentrated membranes on top of the 60% sucrose layer was harvested. These concentrated membranes were then dialyzed extensively against 20 mM Tris (pH 8.0) to remove residual sucrose, before aliquoting and freezing.

YM210W RCs were purified as described in detail previously for wild-type RCs (Swainsbury et al. 2014). In brief, after breakage of bacterial cells and clearing of cell debris, as above, RCs were isolated from membranes in the supernatant using n-dodecyl-N,N-dimethylamine-N-oxide (LDAO) at 1.5% and NaCl at 200 mM. Membrane debris was removed by ultracentrifugation (38,000 rpm, 4 °C, 30 min) and solubilized RCs were then purified by nickel affinity chromatography followed by gel filtration chromatography (Swainsbury et al. 2014). During the latter step, the RC was detergent exchanged into n-dodecyl β-D-maltoside (β-DDM) by running the column in 20 mM Tris (pH 8)/0.04% β-DDM. Fractions with a ratio of protein absorbance at 280 nm to BChl absorbance at 802 nm of less than 1.3 were pooled, and the protein was concentrated using 100 kDa Vivaspin concentrators (GE Healthcare).

Protein and membrane samples were stored at –78 °C until used. Defrosted concentrated samples were diluted before experiments with 20 mM Tris/0.04% β-DDM (pH 7.8) to obtain an optical density of ≤ 0.1 at the maximum of the *P* band around 865 nm (see the relevant absorption spectrum in Fig. 1b) in the sample cell to avoid emission reabsorption effects. More concentrated samples (optical density up to 0.3) were used in some measurements to achieve a

larger signal. In order to compensate for bleaching of the special pair under intense laser excitation, in some experiments, 5 mM sodium ascorbate ($C_6H_7O_6Na$) and 25 µM PMS were added to the buffer solution. This has long been considered to provide a way to imitate a photoactive RC state (see, e.g., (Borisov et al. 1984) for a review).

High-pressure Barospectroscopy

A 0.35-mm-thick stainless steel gasket with 0.3 mm diameter orifice was used to contain the sample between the anvils of a diamond anvil cell (DAC) (D-02, Diacell Products Ltd.), as recently described (Kangur et al. 2017; Timpmann et al. 2017). Pressure applied at an average rate of 100 – 200 bar/minute was determined optically using a ruby-microbead pressure sensor (RSA Le Rubis SA) directly mounted into the sample volume. The precision of the pressure measurements was ± 100–200 bar. The temperature of the DAC was maintained at 23 ± 0.5 °C using a Haake F3 thermostat.

Steady-state transmission and emission spectra were measured with a resolution of 1 nm via a 0.6 m spectrograph (DTMc300, Bentham Instruments Ltd)) equipped with a thermo-electrically cooled CCD camera (DU416A-LDC-DD, Andor Technology). A blackbody tungsten light source BPS100 (BWTek) and a Ti:sapphire laser (3900S, Spectra Physics) were applied in absorption and emission measurements, respectively. Emission spectra were corrected for the spectral sensitivity of the set-up. Absorption spectra (A) were evaluated from the measured transmission spectra (T) as: $A = -\log(T)$. The spectral lineshapes were characterized by two parameters: peak position and width. The width was defined as the full width of the spectral band in frequency scale determined at half maximum intensity.

The emission decay kinetics were measured in transmission mode (i.e., exciting through the back side of the DAC and collecting the signal from its front face) with direct excitation into the lowest energy *P* absorbance band. A tunable femtosecond pulsed Ti: Sapphire laser (Coherent Mira Optima 900-F) with a pulse temporal/spectral width of 100 fs/ 7 nm and repetition rate of 3.8 MHz was used. No recording wavelength dependence of the kinetics was observed in control measurements performed at ambient pressure. Emission was thus recorded broadband, through a long pass filter (TLP01-887, AHF Analysentechnik), using a time-correlated single-photon counting system (SPC-150, Becker & Hickl GmbH) equipped with an avalanche photodiode (ID 100–50, ID Quantique). The fluorescence kinetics were analyzed using Spectra Solve (Version 2.0, LASTEK Pty. Ltd) software and an experimentally determined temporal response function of the set-up (see Fig. 4). Due to multi-exponential kinetics with decay

constants spread from tens of picoseconds to several nanoseconds, two recording time windows of 3.2 ns and 16.0 ns were typically used.

In the case of samples without ascorbate/PMS, a reasonable compromise between the achievable signal-to noise ratio and robustness of the samples with respect to exposure to high laser irradiation doses had to be found by separate measurements. According to our estimates, at the thus chosen excitation intensities 60–40% of the RCs were open. No significant change in the emission kinetics was noticed when the intensity or the data collection time (from tens of seconds to tens of minutes in different measurements) was varied around the selected range. Three independent measurements for every sample were carried out to ensure reproducibility of the data. Reversibility of the pressure effects was confirmed by a recovery of the original spectra and kinetics upon the release of pressure.

RESULTS

Impact of High Pressure on Steady-state Spectra

Near-infrared absorption and emission spectra of the membrane-bound YM210W RCs recorded at different indicated pressures are shown in Fig. 1b. Equivalent spectra for the purified complexes were very similar (data not shown). Please note that henceforth, the detergent-isolated and membrane-bound RCs are for convenience indicated as “i- ” and “m- ” RCs, respectively. The absorption spectra comprised three main bands associated with the Q_y transitions of the BChl and BPhe cofactors. The longest wavelength *P* band that at 1 bar peaks at 870 nm is ascribed to the lowest exciton state of the special pair, which is a π-stacked structure of two BChl molecules. The *B* band at 807 nm is attributed mainly to the two accessory BChls (B_A and B_B) and the *H* band at 756 nm to the two BPhes (H_A and HB) (Brederode et al. 1997). In the wild-type i-RC at ambient pressure, these peaks are correspondingly found at 868, 804, and 758 nm (Hoff and Deisenhofer 1997).

In agreement with the previous measurements on various RCs (Kangur et al. 2017; Timpmann et al. 2017), the three absorption bands universally shifted towards longer wavelengths (red shift) and broadened with increasing pressure. The shift and broadening rates (slopes of the dependences) were the greatest for the P band, followed by the H and B bands (Gall et al. 2001). In fully functional RCs, any emission is associated with the special pair. Therefore, as follows, we will only deal with the effects of pressure on the conjugate *P* absorption and emission spectra.

As can be seen in Fig. 2, pressure dependences of the *P* absorption and emission band positions plotted on an energy scale were generally rather similar, albeit far from being either identical or monotonous. In both i- (Fig. 2a) and m- (Fig. 2b) RCs, the initial close to linear red shift of spectral bands was at intermediate pressures replaced by a blue shift (absorption) or a close to no shift dependence (emission), only to then continue as a quasi-linear red shift at still higher pressures. The slopes of initial and final red shifts were different, the former being slightly greater than the latter. The pressure dependences of the bandwidths were equally intricate. They rapidly broadened between ~ 1.5/3 kbar and ~ 5/7 kbar in i-/m-RCs, respectively, while outside this range the changes were much more moderate.

Comparable spectral behavior has previously been observed in a number of wild-type and engineered RC complexes (Kangur et al. 2017; Timpmann et al. 2017) as well as in peripheral LH2 (Kangur et al. 2008) and core LH1 (Freiberg 2012) light-harvesting complexes from purple photosynthetic bacteria. In all these cases, the correlated modifications of spectral band shape could be associated with pressure-induced ruptures of H-bonds that stabilize BChl cofactors in their protein binding pockets. Recent establishment (Golub et al. 2019) by high-pressure inelastic neutron scattering of increased flexibility of the structure of the LH2 complex in the picosecond time range resulting from the breakage of tertiary structure H-bonds corroborates this conclusion.

The average widths of the absorption and emission spectra obtained at 1 bar were 838 ± 15 cm^{-1} and 876 ± 7 cm^{-1}, respectively, for m-RCs, and 927 ± 25 cm^{-1} and 869 ± 58 cm^{-1}, respectively, for i-RCs. The absorption data reasonably indicated a greater heterogeneity in the more processed purified RC sample, whose spectra were contributed to by RCs with both broken and intact H-bonds. This enlarged heterogeneity is not manifest in emission because, as shown in (Jalviste et al. 2020), the RCs with broken H-bonds appear significantly quenched. The commonly observed diverse endurance against high pressure of photosynthetic pigment–protein complexes (Kangur et al. 2008; Freiberg 2012; Timpmann 2017) also explains the rather different pressure behavior of absorption and emission band shapes seen in Fig. 2. This is because although all the RCs donate to the absorption spectrum, only the most robust (least quenched) sub-population is contributing into the emission spectrum (Jalviste et al. 2020).

Despite a general similarity between the pressure dependences of the i- and m-RCs, there were also notable differences. Most importantly, the intermediate pressure phase in the m-RC was shifted by about 2.5 kbar toward higher pressures compared with that in the i-RC. This can be taken as evidence for the fact that lipids provide more effective protection for the protein against the polar aqueous solvent than detergent molecules in the micelle belt surrounding a

purified complex. A more rapid emission quenching in i-RCs, which, according to a work in progress parallels with a change in hydration status of the C– and N–termini of the protein transmembrane helices, corroborates this notion. In addition, the pressure-induced changes perceived in i-RCs were significantly more marked compared to those in m-RCs. This may be an effect of a higher density (i.e., lower compressibility) of the m-RC due to its relatively more elevated H-bond break pressure.

Recovery of the steady-state spectra also revealed characteristic differences in the behavior of i– and m-RCs (see gray/cyan symbols in Fig. 2). The recovery was practically completed in the case of membrane-protected RCs (Fig. 2b) but rather poor for detergent-purified RCs (Fig. 2a). The overly large discrepancy observed between the original and recovered widths in the i-RC absorption spectrum compared with that between band positions implies a large deformation of the absorption band shape. These observations once again not only emphasize the large stabilizing role of the membrane, but also stress the basic fact that absorption and emission line shapes of RCs convey individual physical information.

Pressure-dependent Emission Decay Kinetics

The decay of emission from either purified or membrane-bound YM210W RCs in the absence of ascorbate/PMS was not mono-exponential. A reasonable fit of the emission kinetics measured at 1 bar (Fig. 3) was obtained by applying at least three exponentially decaying components: a fast picosecond (τ_1), slow picosecond (τ_2) and nanosecond component (τ_3). As shown in Table 1, τ_1 greatly dominated the decay process in both samples (with a relative amplitude close to 90%), while the amplitude contribution of τ_3 was rather marginal at ≤ 0.5%. The remaining component held an intermediate position both in terms of lifetime (~ 200 ps) and amplitude (~ 10%). The most notable effect of the presence of ascorbate/PMS was a growth in the significance of long nanosecond components. The values in Table 1 reasonably agree with transient absorption spectroscopy data available in the literature (Nagarajan et al. 1993; Beekman et al. 1996; Pawlowicz et al. 2010), although the latter lifetimes appear systematically shorter.

DISCUSSION

The following discussion is based on a simplified two-state kinetic scheme (1), which explains the decay of the excited singlet state of the special pair (*P**) in terms of photochemical

(charge separation) and non-photochemical (radiative decay, internal conversion, inter-system crossing) channels/mechanisms:

$$\overset{k_0}{\leftarrow} \mathrm{P}^* \underset{k_2}{\overset{k_1}{\rightleftharpoons}} \mathrm{P}^+\mathrm{H}_A{}^- Q_A \overset{k_3}{\rightarrow} \qquad (1)$$

In scheme (1), the decay of the P^* state population by all non-photochemical routes is described by a single rate constant k_0, the charge separation process $P^* \rightarrow P^+H_A^-$ by k_1, the charge recombination process $P^* \leftarrow P^+H_A^-$ by k_2, and electron transfer to the first quinone acceptor (Q_A) by k_3. Parameter k_2 thus accounts for the observed non-monoexponential decay of P^*. This charge recombination process—a source of a delayed (recombination) emission—normally proceeds uphill in energy and is made available by thermal bath activation. The corresponding standard free energy difference between the P^+H^- and P^* states (the gap) is denoted as $-\Delta G^0$.

The same model was recently applied for analysis of pressure-dependent emission kinetics in purified RCs in the absence of ascorbate/PMS (Jalviste et al. 2020). Based on this original analysis, which implicitly considers that the first experimentally distinguishable charge-separated state in the YM210W RC is P^+H^- rather than the very short-lived P^+B^- as in the wild-type RC (Nagarajan et al. 1993; Pawlowicz et al. 2010; Dominguez et al. 2014) and also misses an explanation for the long nanosecond lifetimes, one may speculate that the experimental τ_1 lifetime in the absence of ascorbate/PMS is largely governed by the photochemistry rate constant k_1 (and to a lesser extent by k_0), while that of τ_2 is governed by k_3 (k_2).

As previously noted (Jalviste et al. 2020), an implicit assumption behind model (1) is a weak dependence on pressure of k_0 relative to other rate constants. In general, all the processes that contribute into the non-photochemical decay rate constant are prone to change with pressure, while only the radiative lifetime dependence has a well-justified predictable form (Olmsted 1976; Hirayama and Phillips 1980; Hirayama et al. 1991).

As can be seen in Table 1, adding ascorbate/PMS at ambient conditions has three major effects on the kinetics: (i) the kinetics could no longer be accounted for by three exponentially decaying components and a fourth long-lifetime component had to be added; (ii) the overall share of nanosecond components increased; and (iii) there was a significant redistribution of relative amplitudes A_1 and A_2 in favor of A_2. Since ascorbate/PMS-treated RCs tend to accumulate reduced primary quinone acceptors under optical excitation, which effectively breaks the electron transfer chain at H_A site, it is our suggestion that the slow nanosecond emission decays are related to a sub-ensemble of RCs with a reduced Q_A. A rather small

amplitude of A_3 in the RCs without ascorbate/PMS then shows that under the weak excitation condition applied, the concentration of such inhibited RCs is negligible. On the other hand, the redistribution of relative amplitudes A_1 and A_2 is, according to our model, evidence for a decreased recombination energy gap in the ascorbate/PMS-treated RC.

Regardless of the qualitative similarity of the i- and m-RC kinetics in the absence of ascorbate/PMS, the data in Table 1 show that in quantitative terms the kinetics are markedly different. Emission by the i-RC fades much more quickly, being also relatively more governed by the τ_1 decay component. The overall slower kinetics of *P** decay in the m-RC are consistent with previous observations on both wild-type and YM210W RCs (Beekman 1996; Schmidt et al. 1993; Vos 1994a). The causes are not known, but are likely related to multiple small differences in the reduction potentials of participating cofactors between membrane-embedded and detergent-solubilized RCs. The rationalization of the increased contribution of the nanosecond component observed in the kinetics of membrane samples follows a similar lead. Accumulation of RCs with reduced Q_A is more likely within a membrane than in solution due to differences in the environment of the RC quinones. A minor difference systematically observed between the intermediate component amplitudes of m- and i-type samples can then be explained by a varied value of the free energy gap in those RCs.

High-pressure compression significantly modified the emission kinetics (see Figs. 3, 4, 5, and 6; similar scales in all figures have been used to aid comparison). Presented in Fig. 4 are the results of a multi-exponential analysis of the emission decay kinetics in ascorbate/PMS-free i- and m-RCs across the whole applied pressure range. They demonstrate that the τ_1 lifetimes decrease nearly exponentially, and almost in parallel to one another, such that the lifetimes measured at 10 kbar are more than two-fold shorter than those recorded at 1 bar. Most notably, these lifetimes that according to scheme (1) are related to the primary charge separation appear systematically greater in m-RCs than in i-RCs. The τ_2 times, which in m-RCs were ~ 40% longer than in i-RCs, slightly increase with pressure. Any discrepancies between nanosecond kinetics are difficult to interpret because of their marginal amplitude contribution.

The pressure-induced variations of amplitudes A_1 and A_2 have opposite signs with A_1 increasing and A_2 decreasing, suggesting a common connection. As a result, in both samples, the decays at high pressures change increasingly to be more single-exponential like, with the τ_1 component accounting for ~96 % (i-RC, no ascorbate/PMS) or 90 % (m-RC, no ascorbate/PMS) of total amplitude. A more detailed analysis performed in the case of purified RCs [46] showed that the A_1 and A_2 amplitudes were undergoing a small (8-9 %) stepwise variation between 1.5 and 3.5 kbar, the pressure range of a H-bond break. Outside this region the amplitudes were almost constant. A roughly similar pattern was

followed for the membrane RC, except that a significant change occurred at almost a 3 kbar higher pressure. The variation was also smoother, such that the high-pressure plateau observed with the i-RC was apparently not achieved even by 10 kbar with the m-RC. The amplitudes of nanosecond components, which according to the above ideas were supposed to correlate with the relative number of RCs in the closed state, either did not change within the experimental uncertainty (i-RC) or slowly increased reaching 3-4% at 4-5 kbar and decreased thereafter (m-RC).

Figures 5 and 6 characterize modifications of the kinetics taking place upon adding ascorbate/PMS. The only prominent pressure-induced change observed for purified RCs was a nearly complete loss past 5–6 kbar of the A_4 amplitude in the ascorbate/PMS-treated sample, see Fig. 5 and Table 1. Other parameter changes were gradual and relatively small (almost within the limits of the experimental uncertainty).

The situation looked quite different for membrane-bound RCs, where already the initial, 1-bar, differences in lifetime and amplitude values appeared greater than in purified complexes, see Fig. 6 and Table 1. Although, as with purified complexes, the emission decay kinetics in the ascorbate/PMS-treated m-RCs turned readily three-exponential past − 5 kbar, interpretation of the relative changes of similar-origin parameters in the two membrane complexes is challenging. Indeed, while the variances between the decay component amplitudes gradually diminished with pressure, they rather abruptly increased past 4 kbar in the case of lifetimes.

The latter effect detected in multiple m-RC samples without ascorbate/PMS looks unique. It was not observed in any other type of sample in this study. Although there is circumstantial evidence for a light-induced conformational modification of the RC structure, which is dependent on pressure, additional studies are required to establish specific origin of this effect.

According to understanding from the model, the significant redistribution of relative amplitudes A_1 and A_2 in favor of A_2 as a result of the addition of ascorbate/PMS can be taken as an evidence for a decreased recombination energy gap in the ascorbate/PMS-treated RC. A gradual increase of A_1 and decrease of A_2 with pressure is then a sign of increasing of the recombination energy gap upon compression in the ascorbate/PMS-treated m-RC complex. In the m-RC without ascorbate/PMS, both A_1 and A_2 remained constant up until 5 kbar, the pressure of the H-bond break in this sample, and then either increased (A_1) or decreased (A_2). Beyond 5 kbar, the amplitude difference between the membrane RCs (i.e., between their recombination energy gaps) turned out to be effectively erased.

The τ_1 and τ_2 lifetimes obtained for the ascorbate/PMS-treated samples at 1 bar appeared systematically longer than those in corresponding untreated samples, see Table 1. At the same time, the scale of their gradual change with pressure was greater (Figs. 5 and 6). As a result, the lifetimes determined in ascorbate/PMS-treated samples at 10 kbar were generally shorter than those determined for samples without ascorbate/PMS.

SUMMARY AND CONCLUDING REMARKS

Electron transfer reactions are ubiquitous in nature, underpinning key biological processes. Here, the dynamical response of primary photochemistry in the *Rba. sphaeroides* RC to hydrostatic compression was investigated at various pressures up to 10 kbar at ambient temperature. The YM210W mutant RC used exhibits a slowed primary charge separation time that allows detailed studies of the kinetics of charge separation by a sensitive picosecond time-resolved single-photon counting technique. As less scattering objects, detergent-purified RC complexes are commonly used in optical spectroscopic studies. In this work, a comprehensive comparison of pressure dependences in detergent-isolated and membrane-embedded RC complexes was performed using membranes from a strain of *Rba. sphaeroides* expressing the YM210W RC but lacking light-harvesting complexes. The effects of adding ascorbate/PMS were also examined as this is often used to maintain open RC conditions under intense excitation light.

The most notable effects of pressure on steady-state absorption/emission spectra were their discontinuous shift and broadening, previously shown to be related with a break of the lone H-bond of the RC special pair. In m-RCs, this break occurs at significantly (2–3 kbar), higher pressures compared with i-RCs, underscoring a stabilizing influence of the membrane environment on the embedded RC protein. In all the samples studied, essential effects of pressure on multi-exponential emission decay kinetics were detected (Figs. 4, 5, and 6). The main change to this kinetics involved a continuous, over two-fold acceleration of the emission decay, which across the 10 kbar pressure range also grew increasingly mono-exponential. The break of the H-bond inferred from steady-state spectra revealed itself in time-resolved measurements via the pressure dependences of the decay kinetics amplitudes (Figs. 4 and 5).

The experimental data were analyzed using a two-level kinetic scheme (1) involving primary charge separation (described by the rate constant (k_1), thermally activated charge recombination to the initial excited state (k_2), electron transfer to a secondary electron acceptor (k_3), and direct (non-photochemical) quenching of the special pair (k_0). Different kinetics were additionally considered in case of the RC with the primary quinone acceptor Q_A unreduced, which

corresponds to the case of an active photosynthesis, or reduced that matches a saturated photosynthesis case. According to such a perfected model (1), the fastest emission decay time basically governed by the rate constant k_1 was significantly greater (by ~ 34% at 1 bar) in the m-RC than in the i-RC. The long picosecond decay component τ_2 was then assigned to the thermally induced recombination emission. The parallel increasing/decreasing trends with pressure of the A_1/A_2 amplitudes could thus be straightforwardly associated with the increasing free energy gap, $-\Delta G^0$, upon protein compression.

An addition of ascorbate/PMS significantly modified the kinetic responses of the samples under high pressure (Figs. 5 and 6). We, therefore, conclude that ascorbate/PMS treatment has several side effects that change the primary photochemistry of bacterial RCs. Overturning a long-standing experimental conjecture, this inference may well justify a critical revision of previous literature in which this treatment was employed.

Acknowledgements

Financial support provided by the Estonian Research Council (grants PRG539, PRG664, and PSG264), the ESF DoRa 4 program (grant NLOFY12523T), and the H2020-MSCA-RISE-2015 program (grant 690853) is greatly appreciated.

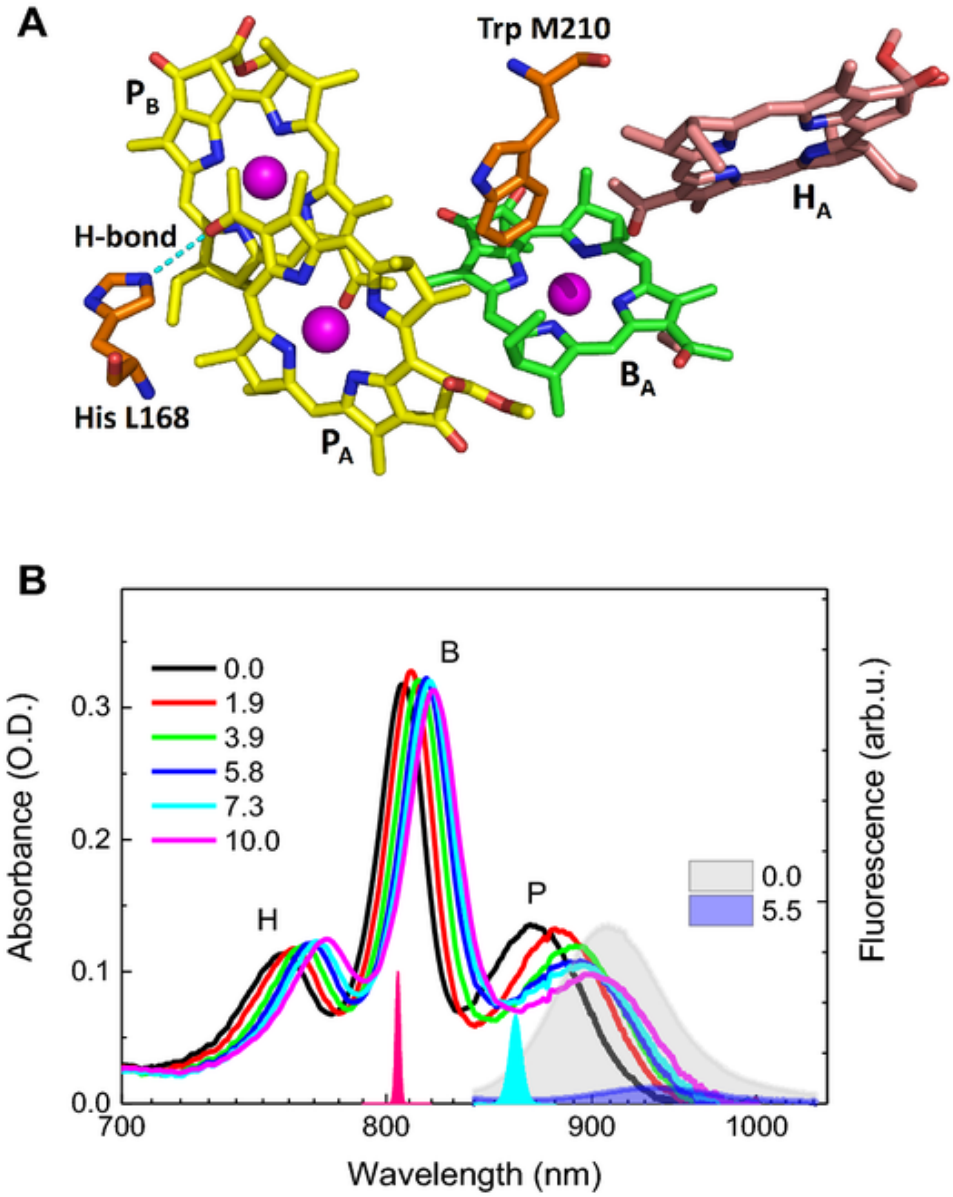

Fig. 1. **a** Structure of the YM210W mutant RC (McAuley et al. 2000). The Trp (orange carbons) is located close to the *P* BChls (yellow carbons), B_A BChl (green carbons), and H_A BPhe (pink carbons). The P_A BChl is H-bonded (cyan dashes) to His L168 (orange carbons). Other atoms are nitrogen (blue), oxygen (red), and magnesium (magenta spheres). **b** Impact of pressure on steady-state absorption and emission spectra of the YM210W m-RC in the presence of ascorbate/PMS. Pressures are in kbar. Common nomenclature of separate absorption bands is displayed. The filled-shape emission spectra excited at 806 nm by a CW laser (lineshape indicated by pink spike of 2 nm width) and corrected for the excitation change on pressure are for clarity presented only at 1 bar (~ 0.0 kbar—gray shading) and 5.5 kbar (blue shading). The cyan pulsed laser excitation line shape peaking at 860 nm used in time-resolved measurements has a width of 7 nm. A reciprocal (linear in energy) wavelength scale is used for better comparison of the absorption and fluorescence spectral shapes and band shifts.

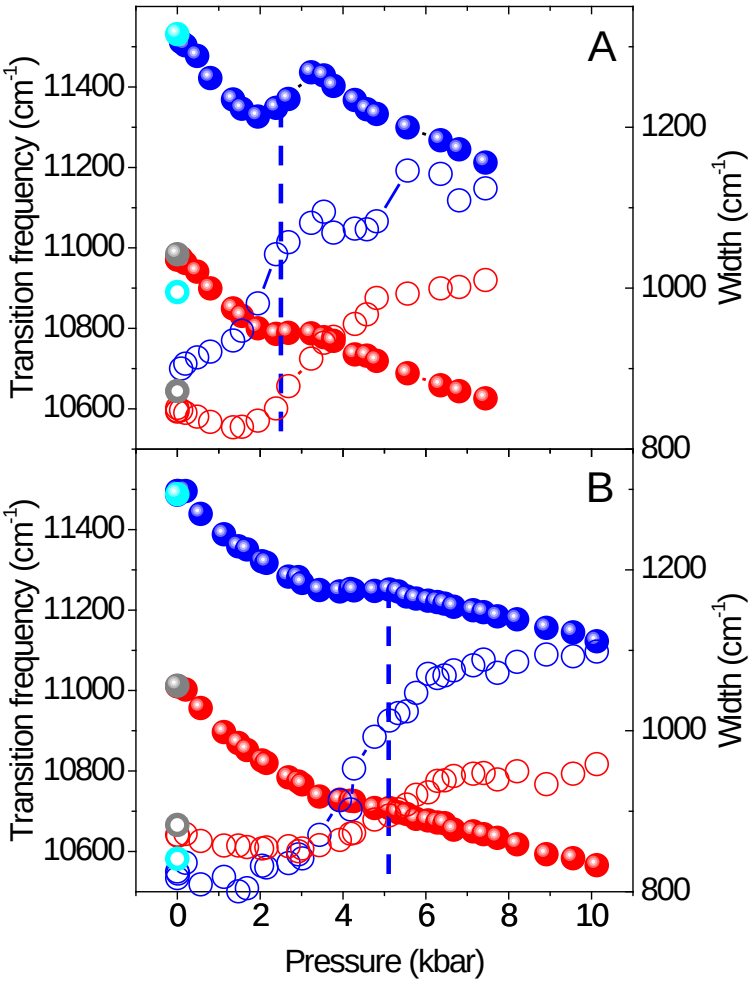

Fig. 2. Impact of high pressure on *P* band absorption (left axis, blue balls) and emission (left axis, red balls) peak energies along with their respective bandwidths (right axis, blue and red open rings) in case of purified **a** and membrane-bound **b** YM210W RC complexes with ascorbate/PMS. Lines connecting the width data are to lead the eye. Differently colored closed and open symbols at ambient pressure designate the data obtained after the pressure release. Vertical dashed lines indicate approximate H-bond break pressures, estimated based on the absorption band shift. See text for further information.

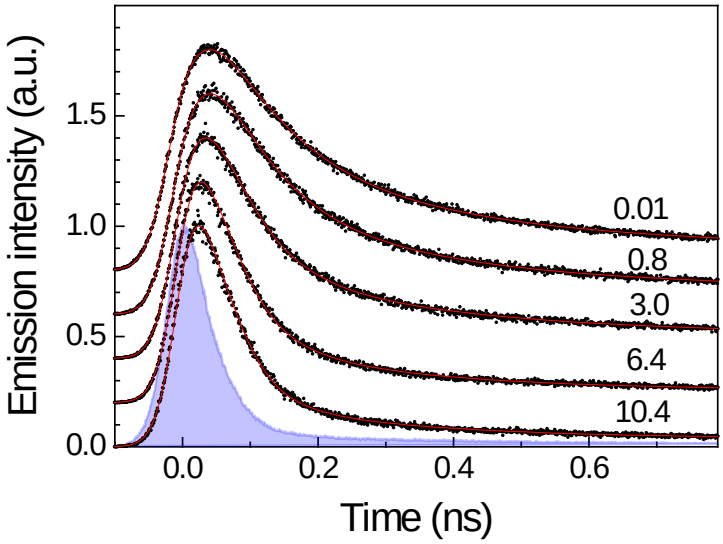

Fig. 3. Emission decay kinetics in the membrane-bound YM210W RC with ascorbate/PMS. The kinetics were obtained with 860-nm excitation and recorded at different indicated pressures in kbar. Traces are arbitrarily offset vertically for comparison. Red solid lines represent four-exponential fits of the scattered experimental data. The blue-filled contour represents the instrument response function

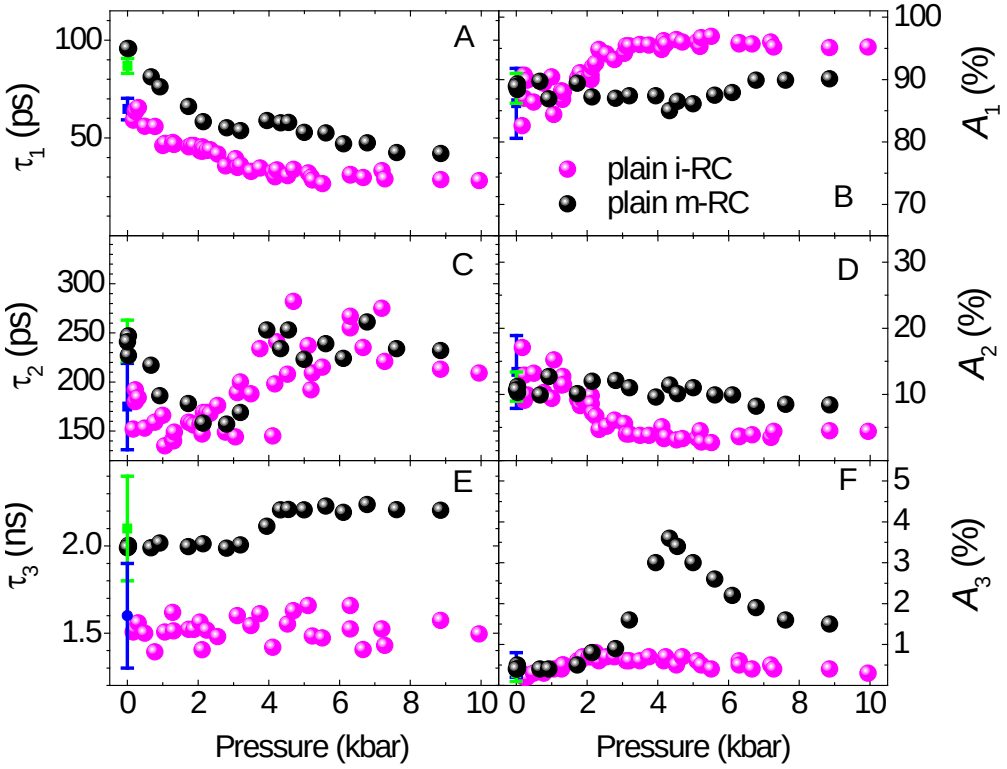

Fig. 4. Comparison of pressure dependences of the emission decay lifetimes (left column) and related relative amplitudes (right column) in ascorbate/PMS-free purified (magenta symbols) and membrane-bound (black symbols) YM210W RCs. Symbols represent data from several independent measurements with 860-nm excitation, directly into the *P* absorption band. Green and blue symbols with uncertainty (standard deviation) denote averaged reference data measured at ambient pressure on, respectively, 10/15 different membrane/purified RC samples in a cuvette. See text for further explanation.

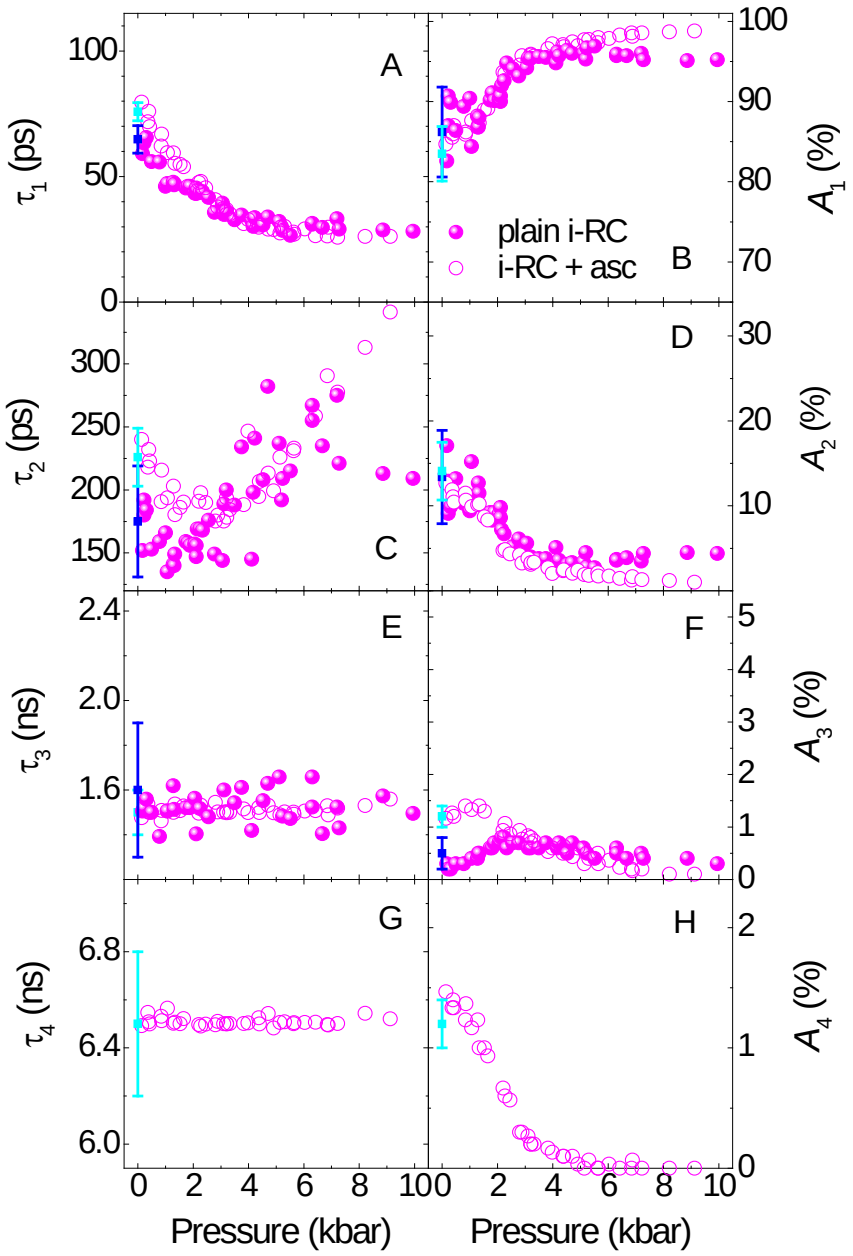

Fig. 5. Comparison of pressure dependences of the emission decay lifetimes (left column) and related relative amplitudes (right column) for the detergent-purified YM210W RC complexes, in the absence of ascorbate/PMS (magenta balls) and the presence of ascorbate/PMS (magenta open rings). Symbols represent data from several independent measurements with 860-nm excitation. Blue and cyan symbols with uncertainty (standard deviation) denote averaged reference data measured at ambient pressure on 15/6 different purified(-ascorbate/PMS)/purified(+ ascorbate/PMS) samples in a cuvette, respectively. See text for further explanation.

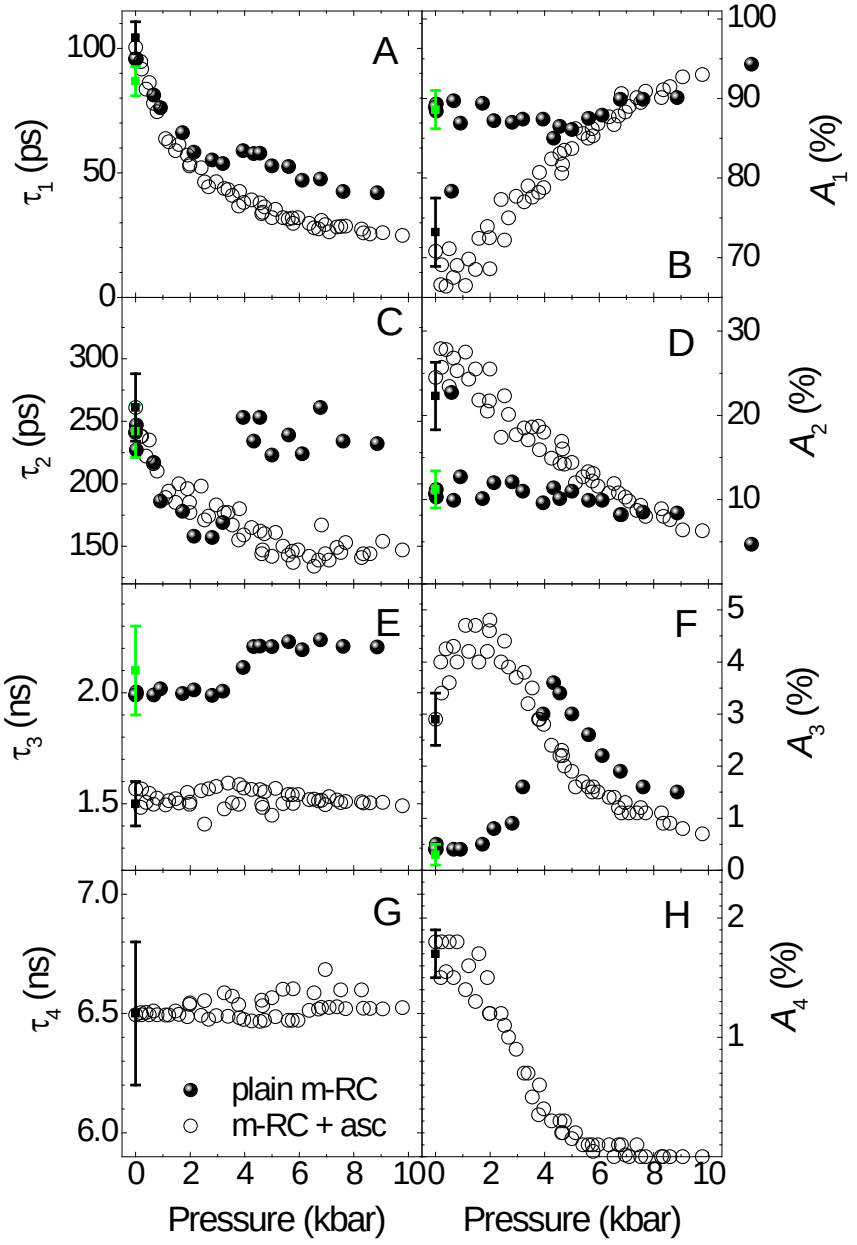

Fig. 6. Comparison of pressure dependences of the emission decay lifetimes (left column) and related relative amplitudes (right column) for the membrane-bound YM210W RC complexes, in the absence (black balls) and the presence (black open rings) of ascorbate/PMS. Symbols represent data from several independent measurements with 860-nm excitation. Green and black symbols with uncertainty (standard deviation) denote averaged reference data measured at ambient pressure on 10/7 different plain membrane (− ascorbate/PMS)/membrane (+ ascorbate/PMS) samples in a cuvette, respectively. See text for further explanation.

Table 1. Fitting parameters (decay times τ_i and relative amplitudes A_i) of the emission decay kinetics in ascorbate/PMS-free and ascorbate/PMS-added purified and membrane-bound YM210W RCs at 1 bar.

Sample		τ_1 (ps) A_1 (%)	τ_2 (ps) A_2 (%)	τ_3 (ps)[a] A_3 (%)	τ_4 (ps)[a] A_4 (%)
Purified RC	-asc	64.8 ± 5.5 86.2 ± 5.6	175 ± 44 13.4 ± 5.5	1600 ± 300 0.5 ± 0.3	-
	+asc	75.8 ± 3.6 83.5 ± 3.4	226 ± 23 14.1 ± 3.4	1500 ± 100 1.2 ± 0.2	6500 ± 300 1.2 ± 0.2
Membrane RC	-asc	86.8 ± 5.8 88.6 ± 2.4	242 ± 21 11.2 ± 2.2	2100 ± 200 0.3 ± 0.2	-
	+asc	104.3 ± 6.4 73.2 ± 4.3	261 ± 27 22.3 ± 4.0	1500 ± 100 2.9 ± 0.5	6500 ± 300 1.7 ± 0.2

[a] Because of low amplitude values and a narrow recording time window, the nanosecond decay times are only approximate.

References

Beekman LMP et al (1995) Time-resolved and steady-state spectroscopic analysis of membrane-bound reaction centers from Rhodobacter sphaeroides: Comparisons with detergent-solubilized complexes. Biochemistry 34(45):14712–14721

Beekman LMP et al (1996) Primary electron transfer in membrane-bound reaction centers with mutations at the M210 position. J Phys Chem 100(17):7256–7268

Beekman LMP et al (1997) Characterization of the light-harvesting antennas of photosynthetic purple bacteria by Stark spectroscopy 2 LH2 complexes: influence of the protein environment. J Phys Chem B 101(37):7293–7301

Blankenship RE (2002) Molecular mechanisms of photosynthesis. Blackwell Science, Oxford

Boonyaratanakornkit BB, Park CB, Clark DS (2002) Pressure effects on intra- and intermolecular interactions within proteins. Biochim Biophys Acta 1595:235–249

Borisov AY, Kotova EA, Samuilov VD (1984) Delayed luminescence of bacteriochlorophyll and primary steps of electron transfer in photosynthetic reaction centers of purple bacteria (review). Mol Biol (Moscow) 18(4):869–891

Borisov AY et al (1985) Kinetics of picosecond bacteriochlorophyll luminescence in vivo as a function of the reaction center state. Biochim Biophys Acta 807(3):221–229

Bowyer JR et al (1985) Photosynthetic membrane development in Rhodopseudomonas sphaeroides: Spectral and kinetic characterization of redox components of light-driven electron flow in apparent photosynthetic membrane growth initiation sites. J Biol Chem 260(6):3295–3304

Clayton RK, Devault D (1972) Effects of high pressure on photochemical reaction centers from Rhodopseudomonas spheroides. Photochem Photobiol 15(2):165–175

Dominguez PN et al (2014) Primary reactions in photosynthetic reaction centers of Rhodobacter sphaeroides – Time constants of the initial electron transfer. Chem Phys Lett 601:103–109

Driscoll B et al (2014) Energy transfer properties of Rhodobacter sphaeroides chromatophores during adaptation to low light intensity. Phys Chem Chem Phys 16(32):17133–17141

Freiberg, A., et al. *Spectral and kinetic effects accompanying the assembly of core complexes of Rhodobacter sphaeroides.* Biochimica et Biophysica Acta (BBA)–Bioenergetics, 2016. 1857(11): p. 1727–1733.

Freiberg A et al (1993) Pressure effects on spectra of photosynthetic light-harvesting pigment-protein complexes. Chem Phys Lett 214(1):10–16

Freiberg A, Rätsep M, Timpmann K (2012) A comparative spectroscopic and kinetic study of photoexcitations in detergent-isolated and membrane-embedded LH2 light-harvesting complexes. Biochem Biophys Acta 1817:1471–1482

Freiberg A et al (2012) Structural implications of hydrogen-bond energetics in membrane proteins revealed by high-pressure spectroscopy. Biophys J 103:2352–2360

Fulcher TK, Beatty JT, Jones MR (1998) Demonstration of the key role played by the PufX protein in the functional and structural organization of native and hybrid bacterial photosynthetic core complexes. J Bacteriol 180(3):642–646

Gall A et al (2001) Effect of high pressure on the photochemical reaction center from Rhodobacter sphaeroides R261. Biophys J 80(3):1487–1497

Gall A et al (2004) The effect of internal voids in membrane proteins: high-pressure study of two photochemical reaction centers from Rhodobacter sphaeroides. FEBS Lett 28121:1–5

Gibasiewicz K et al (2011) Mechanism of recombination of the P+HA– radical pair in mutant Rhodobacter sphaeroides reaction centers with modified free energy gaps between P+BA– and P+HA–. J Phys Chem B 115(44):13037–13050

Gibasiewicz K et al (2013) Analysis of the temperature-dependence of P+HA− charge recombination in the Rhodobacter sphaeroides reaction center suggests nanosecond temperature-independent protein relaxation. Phys Chem Chem Phys 15(38):16321–16333

Gibasiewicz K et al (2016) Weak temperature dependence of P+HA−recombination in mutant Rhodobacter sphaeroides reaction centers. Photosynth Res 128(3):243–258

Godik VI, Borisov AY (1979) Short-lived delayed luminescence of photosynthetic organisms: I: nanosecond afterglows in purple bacteria at low redox potentials. Biochim Biophys Acta 548(2):296–308

Godik VI, Borisov AY (1980) Short-lived delayed luminescence of photosynthesizing organisms: II: the ratio between delayed and prompt fluorescence as studied by the modulation method. Biochim Biophys Acta 590(2):182–193

Golub M et al (2019) Picosecond dynamical response to a pressure-induced break of the tertiary structure hydrogen bonds in a membrane chromoprotein. J Phys Chem B 123(9):2087–2093

Hirayama S, Phillips D (1980) Correction for refractive index in the comparison of radiative lifetimes in vapour and solution phases. J Photochem 12(2):139–145

Hirayama S et al (1991) Effect of pressure on the natural radiative lifetimes of anthracene derivatives in solution. J Phys Chem 95(8):2971–2975

Hoff AJ, Deisenhofer J (1997) Photophysics of photosynthesis: structure and spectroscopy of reaction centers of purple bacteria. Phys Rep 287(1):1–247

Hunter, C.N., et al. eds. *The purple phototrophic bacteria*: advances in photosynthesis and respiration. Vol. 28. 2008, Springer: Dordrecht, The Netherlands.

Hunter CN, Kramer HJM, Van Grondelle R (1985) Linear dichroism and fluorescence emission of antenna complexes during photosynthetic unit assembly in Rhodopseudomonas sphaeroides. Biochim Biophys Acta 807(1):44–51

Jalviste, E., et al. *High-pressure modulation of primary photosynthetic reactions.* J Phys Chem B, 2020.

Jonas J, DeFries T, Wilbur DJ (1976) Molecular motions in compressed liquid water. J Chem Phys 65:582–588

Jones MR et al (1992a) Construction and characterization of a mutant of Rhodobacter sphaeroides with the reaction center as the sole pigment-protein complex. Biochemistry 31(18):4458–4465

Jones MR et al (1992b) Mutants of Rhodobacter sphaeroides lacking one or more pigment-protein complexes and complementation with reaction-centre, LH1, and LH2 genes. Mol Microbiol 6(9):1173–1184

Jones MR et al (1994) Site-specific mutagenesis of the reaction center from Rhodobacter sphaeroides studied by Fourier transform Raman spectroscopy: mutations at tyrosine M210 do not affect the electronic structure of the primary donor. FEBS Lett 339(1–2):18–24

Kangur L, Timpmann K, Freiberg A (2008) Stability of integral membrane proteins against high hydrostatic pressure: The LH2 and LH3 antenna pigment-protein complexes from photosynthetic bacteria. J Phys Chem B 112:7948–7955

Kangur L, Jones MR, Freiberg A (2017) Hydrogen bonds in the vicinity of the special pair of the bacterial reaction center probed by hydrostatic high-pressure absorption spectroscopy. Biophys Chem 231:27–33

Leiger K et al (2007) Pressure-induced spectral changes for the special-pair radical cation of the bacterial photosynthetic reaction center. J Chem Phys 126(21):215102

McAuley KE et al (2000) X-ray crystal structure of the YM210W mutant reaction centre from Rhodobacter sphaeroides. FEBS Lett 467(2–3):285–290

Müller P et al (1996) The internal conversion rate of the primary donor in reaction centers of Rhodobacter sphaeroides. Berichte der Bunsengesellschaft für physikalische Chemie 100(12):1967–1973

Nagarajan V et al (1993) Kinetics and free energy gaps of electron-transfer reactions in Rhodobacter sphaeroides reaction centers. Biochemistry 32(46):12324–12336

Olmsted J (1976) Effect of refractive index on molecular radiative lifetimes. Chem Phys Lett 38(2):287–292

Pajusalu M et al (2019) High-pressure control of photosynthetic excitons. Chem Phys 525:110404

Pawlowicz NP et al (2010) An investigation of slow charge separation in a Tyrosine M210 to Tryptophan mutant of the Rhodobacter sphaeroides reaction center by femtosecond mid-infrared spectroscopy. Phys Chem Chem Phys 12(11):2693–2705

Pflock T et al (2008) Comparison of the fluorescence kinetics of detergent-solubilised and membrane-reconstituted LH2 complexes from Rps: acidophila and Rb sphaeroides. Photosynth Res 95:291–298

Pugh, R.J., et al. *The LH1–RC core complex of Rhodobacter sphaeroides: interaction between components, time-dependent assembly, and topology of the PufX protein.* Biochimica et Biophysica Acta (BBA)—Bioenergetics, 1998. 1366(3): p. 301–316.

Redline NL, Windsor MW (1992) The effect of pressure on charge separation in photosynthetic bacterial reaction centers of Rhodopseudomonas viridis. Chem Phys Lett 198(3–4):334–340

Redline NL, Windsor MW, Menzel R (1991) The effect of pressure on the secondary (200 ps) charge transfer step in bacterial reaction centers of Rhodobacter sphaeroides R-26. Chem Phys Lett 186(2–3):204–209

Scharnagl C, Reif M, Friedrich J (2005) Stability of proteins: temperature, pressure and the role of the solvent. Biochim Biophys Acta 1749:187–213

Schmidt, S., et al. *Time-resolved spectroscopy of the primary photosynthetic processes of membrane-bound reaction centers from an antenna-deficient mutant of Rhodobacter capsulatus.* Biochimica et Biophysica Acta (BBA)—Bioenergetics, 1993. 1144(3): p. 385–390.

Silva JL, Weber G (1993) Pressure stability of proteins. Annu Rev Phys Chem 44:89–113

Swainsbury DJK et al (2014) Evaluation of a biohybrid photoelectrochemical cell employing the purple bacterial reaction centre as a biosensor for herbicides. Biosens Bioelectron 58:172–178

Timpmann K, et al. High pressure induced acceleration of primary photochemistry in membrane-bound wild type and mutant bacterial reaction centres, in Ultrafast phenomena in Spectroscopy, R. Kaarli, A. Freiberg, and P. Saari, (eds) (1998) Institute of Physics. Tartu, University of Tartu, pp 236–247

Timpmann K, Woodbury NW, Freiberg A (2000) Unraveling exciton relaxation and energy transfer in LH2 photosynthetic antennas. J Phys Chem B 104(42):9769–9771

Timpmann K et al (2017) High-pressure modulation of the structure of the bacterial photochemical reaction center at physiological and cryogenic temperatures. J Phys B: At Mol Opt Phys 50(14):144006

Urboniene V et al (2007) Solvation effect of bacteriochlorophyll excitons in light-harvesting complex LH2. Biophysical J 93:2188–2198

Van Brederode ME et al (1997) A new pathway for transmembrane electron transfer in photosynthetic reaction centers of Rhodobacter sphaeroides not involving the excited special pair. Biochemistry 36(23):6855–6861

Van Brederode ME, Jones MR, Van Grondelle R (1997) Fluorescence excitation spectra of membrane-bound photosynthetic reaction centers of Rhodobacter sphaeroides in which the tyrosine M210 residue is replaced by tryptophan: evidence for a new pathway of charge separation. Chem Phys Lett 268(1):143–149

van Brederode ME et al (1999) Multiple pathways for ultrafast transduction of light energy in the photosynthetic reaction center of Rhodobacter sphaeroides. Proc Natl Acad Sci USA 96(5):2054–2059

Vos MH et al (1994a) Influence of the membrane environment on vibrational motions in reaction centres of Rhodobacter sphaeroides. Biochim Biophys Acta 1186:117–122

Vos MH et al (1994b) Coherent Dynamics during the primary electron-transfer reaction in membrane-bound reaction centers of Rhodobacter sphaeroides. Biochemistry 33(22):6750–6757

Williams JC, Steiner LA, Feher G (1986) Primary structure of the reaction center from Rhodopseudomonas sphaeroides. Proteins Struct Funct Genet 1(4):312–325

Windsor MW, Menzel R (1989) Effect of pressure on the 12 ns charge recombination step in reduced bacterial reaction centers of Rhodobacter sphaeroides R-26. Chem Phys Lett 164(2–3):143–150